5-1-2018

# Sequence Stratigraphy, Chemostratigraphy and Facies Analysis of Cambrian Series 2 - Series 3 Boundary Strata in Northwestern Scotland

Luke E. Faggetter
*University of Leeds*

Paul B. Wignall
*University of Leeds*

Sara B. Pruss
*Smith College*, spruss@smith.edu

Yadong Sun
*Friedrich-Alexander-Universität Erlangen-Nürnberg*

Robert J. Raine
*Geological Survey of Northern Ireland*

*See next page for additional authors*

*Geol. Mag.* **155** (*4*), *2018, pp. 865–877.* © *Cambridge University Press 2016*
doi:10.1017/S0016756816000947


# Sequence stratigraphy, chemostratigraphy and facies analysis of Cambrian Series 2 – Series 3 boundary strata in northwestern Scotland

LUKE E. FAGGETTER*†, PAUL B. WIGNALL*, SARA B. PRUSS‡, YADONG SUN§¶, ROBERT J. RAINE||, ROBERT J. NEWTON*, MIKE WIDDOWSON#, MICHAEL M. JOACHIMSKI§ & PAUL M. SMITH**

*School of Earth and Environment, University of Leeds, Woodhouse Lane, Leeds, LS2 9JT, United Kingdom
‡Smith College, Department of Geosciences, Northampton, Massachusetts 01063, USA
§GeoZentrum Nordbayern, Universität Erlangen-Nürnberg, Schlossgarten 5, 91054 Erlangen, Germany
¶State Key Laboratory of Geobiology and Environmental Geology, China University of Geosciences, Wuhan, 430074, P.R. China
||Geological Survey of Northern Ireland, Dundonald House, Upper Newtownards Road, Ballymiscaw, Belfast, BT4 3SB, United Kingdom
#Department of Geography, Earth and Environmental Sciences (GEES), University of Hull, Hull HU6 7RX, United Kingdom
**Oxford University Museum of Natural History, Parks Road, Oxford, OX1 3PW, United Kingdom

(*Received* 21 March 2016; *accepted* 5 September 2016; *first published online* 4 November 2016)

**Abstract** – Globally, the Series 2 – Series 3 boundary of the Cambrian System coincides with a major carbon isotope excursion, sea-level changes and trilobite extinctions. Here we examine the sedimentology, sequence stratigraphy and carbon isotope record of this interval in the Cambrian strata (Durness Group) of NW Scotland. Carbonate carbon isotope data from the lower part of the Durness Group (Ghrudaidh Formation) show that the shallow-marine, Laurentian margin carbonates record two linked sea-level and carbon isotopic events. Whilst the carbon isotope excursions are not as pronounced as those expressed elsewhere, correlation with global records (Sauk I – Sauk II boundary and *Olenellus* biostratigraphic constraint) identifies them as representing the local expression of the ROECE and DICE. The upper part of the ROECE is recorded in the basal Ghrudaidh Formation whilst the DICE is seen around 30 m above the base of this unit. Both carbon isotope excursions co-occur with surfaces interpreted to record regressive–transgressive events that produced amalgamated sequence boundaries and ravinement/flooding surfaces overlain by conglomerates of reworked intraclasts. The ROECE has been linked with redlichiid and olenellid trilobite extinctions, but in NW Scotland, *Olenellus* is found after the negative peak of the carbon isotope excursion but before sequence boundary formation.

Keywords: Durness Group, ROECE, DICE, trilobite extinction, Scotland.

## 1. Introduction

The Series 2 – Series 3 transition in the Cambrian System coincides with the first biotic crisis of the Phanerozoic, which saw major losses amongst the archaeocyathid sponges and two major trilobite groups, the redlichiids and olenellids (Palmer, 1998; Zhu *et al*. 2004; Zhu, Babcock & Peng, 2006; Guo *et al*. 2010; Fan, Deng & Zhang, 2011; Wang *et al*. 2011; Zhang *et al*. 2013; Ishikawa *et al*. 2014). Around the same time, a series of major carbon isotope oscillations have been recorded including a major negative $\delta^{13}C$ excursion thought to coincide with the trilobite extinctions (Montañez *et al*. 2000; Zhu *et al*. 2004; Zhu, Babcock & Peng, 2006; Wang *et al*. 2011; Peng, Babcock & Cooper, 2012). The event has therefore been termed the Redlichiid–Olenellid Extinction Carbon Isotope Excursion (ROECE) (Zhu *et al*. 2004; Zhu, Babcock & Peng, 2006; Álvaro *et al*. 2008; Guo *et al*. 2010; Fan, Deng & Zhang, 2011; Wang *et al*. 2011).

The ROECE is also contemporaneous with a major regression–transgression couplet responsible for the boundary between the Sauk I and Sauk II supersequences of the Laurentian continent (Sloss, 1963; Palmer & James, 1980; McKie, 1993; Raine & Smith, 2012). However, this sea-level change does not have an expression outside of Laurentia and, thus, has no apparent effect in Gondwana (Pratt & Bordonaro, 2014) or South China (Zhu *et al*. 2004). In contrast, its Laurentian expression is a major hiatus in shelf locations, whilst down-dip a thick lowstand package is seen, such as the Hawke Bay Formation of Newfoundland; the regression has therefore been referred to as the 'Hawke Bay event' (Palmer & James, 1980).

The relationship between extinctions, sea-level change and carbon isotope excursions is a common theme in studies of environmental crises, but their interplay at this time in the Cambrian Period is unclear.

†Author for correspondence: ee08lef@leeds.ac.uk

Originally it was suggested that there were two crises: the Sinsk event (Zhuravlev & Wood, 1996), named after the widespread development of black shales in Siberia, which especially affected archaeocyathans; and a later, severe extinction of redlichiid and olenellid trilobites coinciding with the regressive Hawke Bay event (Palmer & James, 1980; Zhuravlev & Wood, 1996). However, others have also related this second crisis to the spread of anoxic waters and a negative shift of carbon isotope values (Zhu *et al.* 2004).

The Cambrian carbonate carbon isotope record experienced multiple oscillations, and correlating these excursions provides potentially the best approach for intercontinental correlation (e.g. Maloof *et al*. 2010; Peng, Babcock & Cooper, 2012; Smith *et al*. 2015). At least two negative excursions occur in the uppermost Cambrian Series 2: the Archaeocyathan Extinction Carbon isotope Excursion (AECE) (Brasier *et al*. 1994; Zhu, Babcock & Peng, 2006) and the ROECE. What remains unclear about both of these isotopic events is their relationship to the extinction events. For example, whilst it is well established that archaeocyathans suffered a major decline at the Sinsk event (Zhuravlev & Wood, 1996), their final disappearance remains unconstrained. In some instances, archaeocyathans are thought to extend closer to the Series 2 – Series 3 boundary (Perejón *et al.* 2012), with a few putative occurrences even known from the Cambrian Series 3 (Debrenne, Rozanov & Webers, 1984). If the archaeocyathans persisted to the Series 2 – Series 3 boundary, the ROECE event may well be coeval with the last occurrence of the archaeocyathans as well as that of the redlichiid and olenellid trilobites.

In Series 3, the base of the Drumian Stage is defined by the first appearance datum (FAD) of the agnostid trilobite *Ptychagnostus atavus*, which, in the Great Basin (USA), is associated with transgression and the Drumian negative carbon isotope excursion (DICE) (Babcock *et al.* 2004, 2007; Zhu, Babcock & Peng, 2006; Howley & Jiang, 2010). The onset of the excursion commonly coincides with the FAD of *P. atavus* (Montañez *et al.* 2000; Babcock *et al.* 2007) and has an amplitude of around −3 ‰ in the Great Basin and Canadian Rockies (Montañez *et al.* 2000; Howley & Jiang, 2010). Elsewhere, however, the excursion is substantially less pronounced. Thus, in the carbonate record of South China (Wang *et al.* 2011) and the organic carbon record of Sweden the DICE is only ∼ 1 ‰ (Ahlberg *et al*. 2009).

In order to further evaluate events around the Series 2 – Series 3 boundary we have conducted a facies and sequence stratigraphical analysis of the transition between the An t-Sròn and Ghrudaidh formations in NW Scotland (Fig. 1). Facies analysis of the Scottish strata shows a major lithological change at this level and recent sequence stratigraphic study has suggested that the formational boundary also correlates with the Sauk I – Sauk II supersequence boundary of North America (Raine & Smith, 2012). To further aid correlation, and in an attempt to identify the $\delta^{13}C$ changes associated with the ROECE and DICE, carbonate and organic carbon isotope results are presented here.

## 2. Geological setting and study locations

An almost continuous belt of Cambro-Ordovician rocks crop out along the Caledonian foreland within the Moine Thrust Zone of northwestern Scotland, from Loch Eriboll in the north to the Isle of Skye in the southwest (Fig. 1; Raine & Smith, 2012). These strata record deposition on the southeastern Laurentian margin and are characterized by the predominance of marine sandstones of the Ardvreck Group and limestones and dolostones of the Durness Group. The Salterella Grit Member of the An t-Sròn Formation forms the uppermost part of the Ardvreck Group and consists of *Skolithos*-bioturbated cross-stratified, quartz arenitic sandstones (McKie, 1989, 1990). The transition to the Ghrudaidh Formation of the Durness Group marks the establishment of a thick succession of dolostone and limestone beds that formed in a range of supratidal, peritidal and shallow-marine carbonate platform deposits (Raine & Smith, 2012). Quartz sand grains persist for a few metres in the basal Ghrudaidh Formation but their disappearance at higher levels has been attributed to an abrupt transgression causing the sediment hinterland to become far distant (Raine & Smith, 2012).

### 2.a. Loch Eriboll (58° 28′ 56.64″ N, 4° 40′ 01.01″ W)

A promontory on the western shore of Loch Eriboll is one of the few localities in NW Scotland in which the An t-Sròn, Ghrudaidh and the lower portion of the Eilean Dubh formations are well exposed without a significant tectonic break (Raine & Smith, 2012). The outcrop spans the upper Pipe Rock Member of the Eriboll Formation through the Fucoid and Salterella Grit members, and the Ghrudaidh Formation to a level above its boundary with the Eilean Dubh Formation.

### 2.b. Ardvreck Castle (58° 10′ 12.51″ N, 4° 59′ 55.00″ W)

A road cutting along the eastern shore of Loch Assynt exposes the upper sections of the Salterella Grit Member, and the transition into the lowest beds of the Ghrudaidh Formation.

## 3. Methods

Detailed sedimentary logging and sample collection was conducted at Loch Eriboll through a 52 m thick section of siliciclastic and carbonate rocks of the Ardvreck and Durness groups. At Ardvreck Castle, a 10 m section spanning the same boundary was also logged. Bed numbers were allocated, and field observations and petrographical analyses were used for lithofacies and fossil identification. SEM analysis (secondary and backscattered imaging and EDX elemental mapping) was undertaken to examine more detailed petrographic features including the nature of the pyrite content.

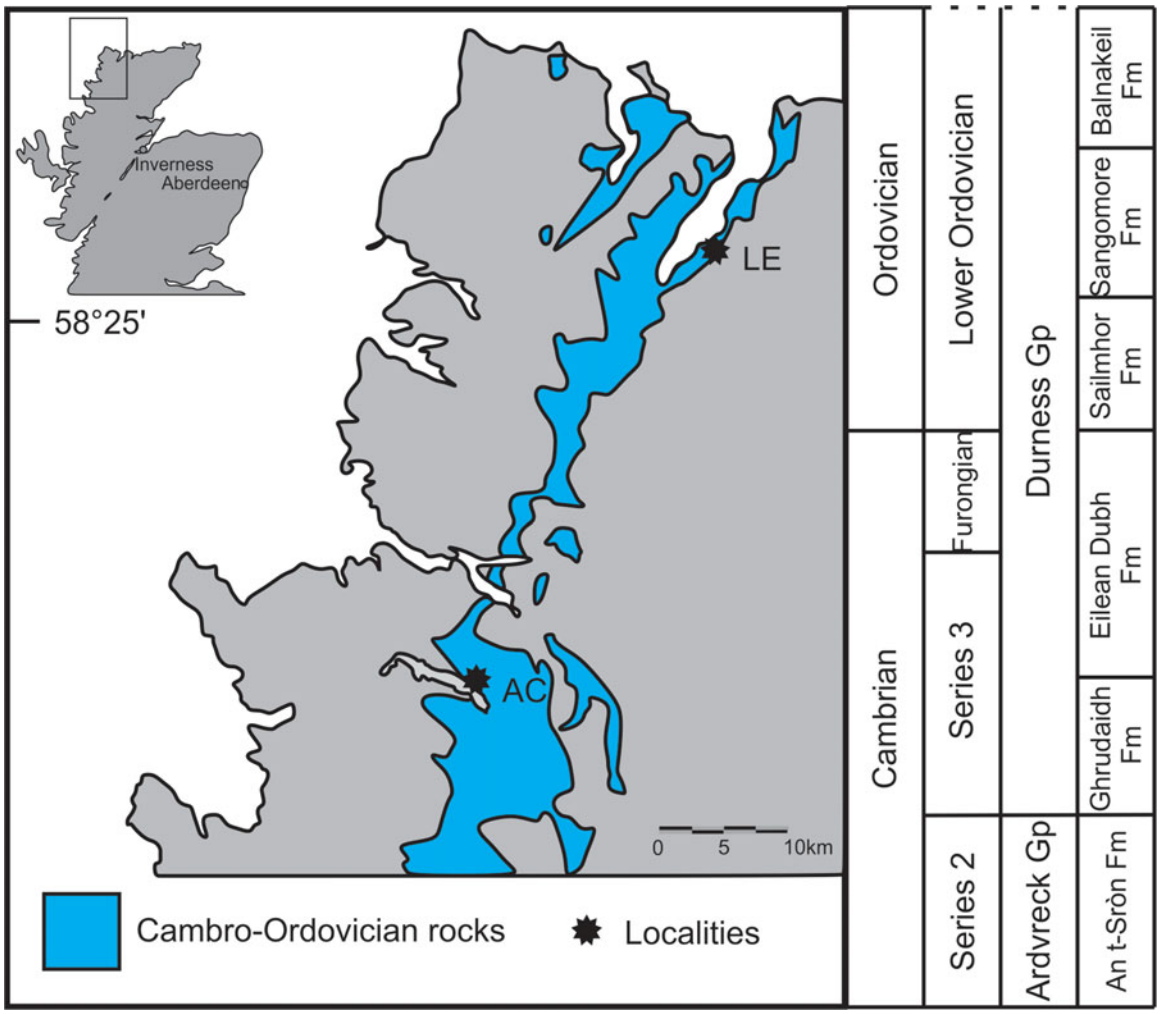


Figure 1. (Colour online) Locality map of the study locations (LE – Loch Eriboll; AC – Ardvreck Castle) in NW Scotland, modified from Raine & Smith (2012), and summary of Lower–Middle Cambrian stratigraphic units in the region.

The $\delta^{13}C_{carb}$ and $\delta^{18}O_{carb}$ were analysed at the GeoZentrum Nordbayern of the FAU Erlangen-Nürnberg, Germany. Carbonate powders were reacted with 100 % phosphoric acid at 70 °C using a Gasbench II connected to a ThermoFisher Delta V Plus mass spectrometer. All values are reported in per mil relative to the VPDB (Vienna Pee Dee Belemnite) by assigning $\delta^{13}C$ and $\delta^{18}O$ values of +1.95 and −2.20 ‰ to international standard NBS19, and −46.6 and −26.4 ‰ to international standard LSVEC, respectively. Reproducibility monitored by replicate analyses of laboratory standards calibrated to NBS19 and LSVEC was ± 0.07 (1 sd) for $\delta^{13}C$ and ± 0.05 (1 sd) for $\delta^{18}O$.

## 4. Facies analysis

### 4.a. Loch Eriboll

#### *4.a.1. Salterella Grit Member*

The 11 m thick Salterella Grit Member consists of beds of medium-grained, cross-bedded and planar and parallel laminated quartz arenites together with strongly bioturbated quartz arenites (‘pipe rock’) with abundant *Skolithos* burrows (Fig. 2). The cross-sets are stacked on low-angle bounding surfaces and in some beds the intensity of *Skolithos* burrows is sufficient to obliterate the bedding, especially in the uppermost levels where the abundance of *Salterella* also increases. Petrographic examination shows the original quartz grains are well sorted and range from well-rounded to sub-rounded (Fig. 3g, h). Also present are thin interbeds of laminated mudstones and fine siltstones that display a cleavage. The contact between these finer beds and overlying sandstone beds commonly displays small gutter casts.

#### *4.a.2. Ghrudaidh Formation*

The Ghrudaidh Formation consists of massive, burrow-mottled and well-bedded dolomite beds that frequently display small vugs. The vugs have been interpreted to record the former presence of gypsum and anhydrite (Raine & Smith, 2012), although they are now partly filled with dolomite rhombs. In the absence of evaporitic pseudomorphs in the vugs, it is also feasible that these features are a remnant of volume reduction during dolomitization. Finely laminated white and dark grey

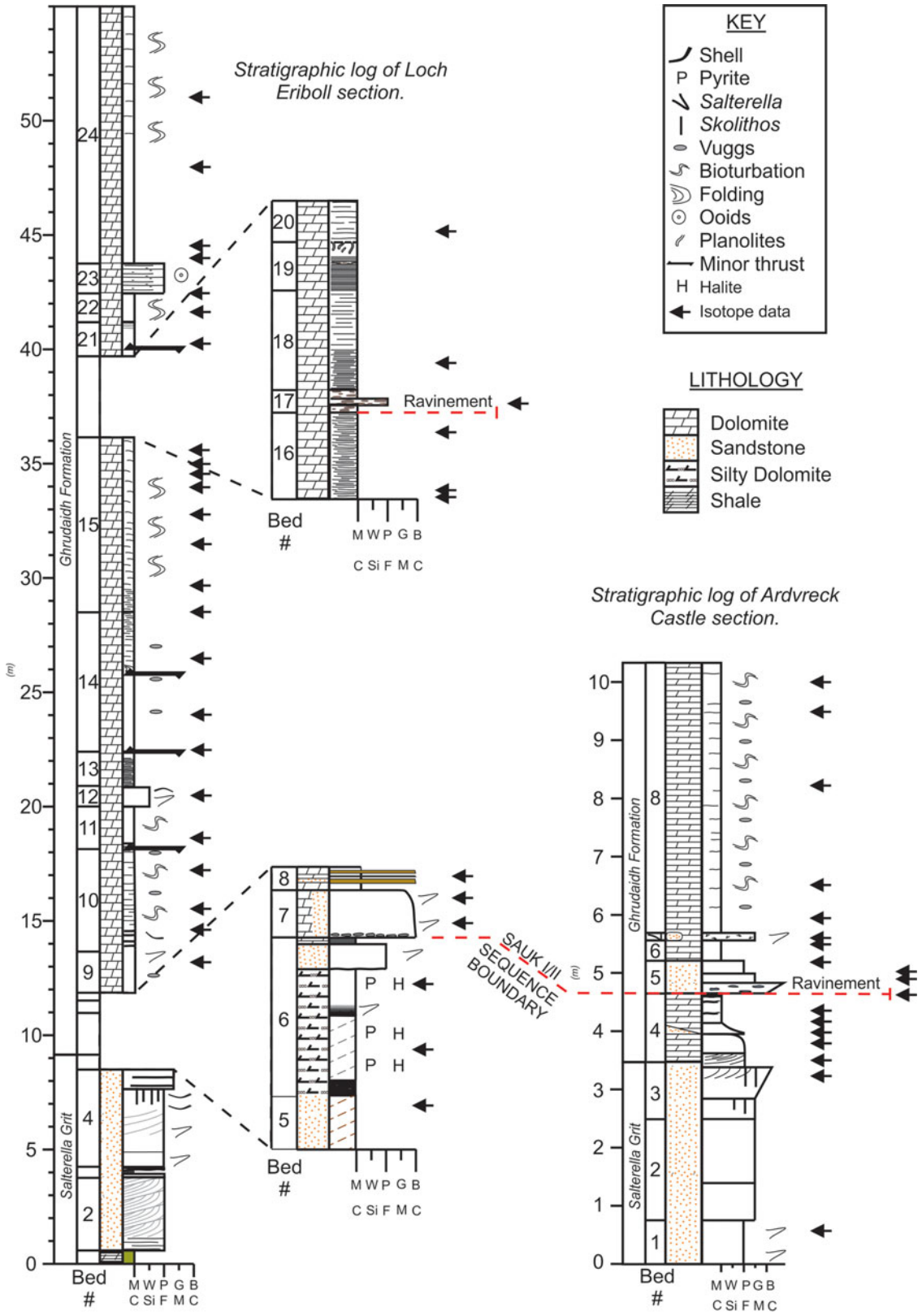


Figure 2. (Colour online) Sedimentary logs of the Loch Eriboll and Ardvreck Castle sections showing the correlation of a ravinement surface near the base of the Ghrudaidh Formation and a second surface ~ 27 m above the base of the formation at Loch Eriboll.

dolomite is also present notably around 27 m above the base of the formation. Towards the top of the section is a ~ 1 m thick (bed LE23) oolitic grainstone bed, a rare coarse-grained horizon. In thin-section the majority of the dolomite beds consist of a mosaic of interlocking dolomite rhombs of silt to sand grade, which have mostly obliterated primary depositional fabrics. Thus, even apparently fine-grained, laminated dolomites seen in the field are found to be dolosparites when seen in thin-section.

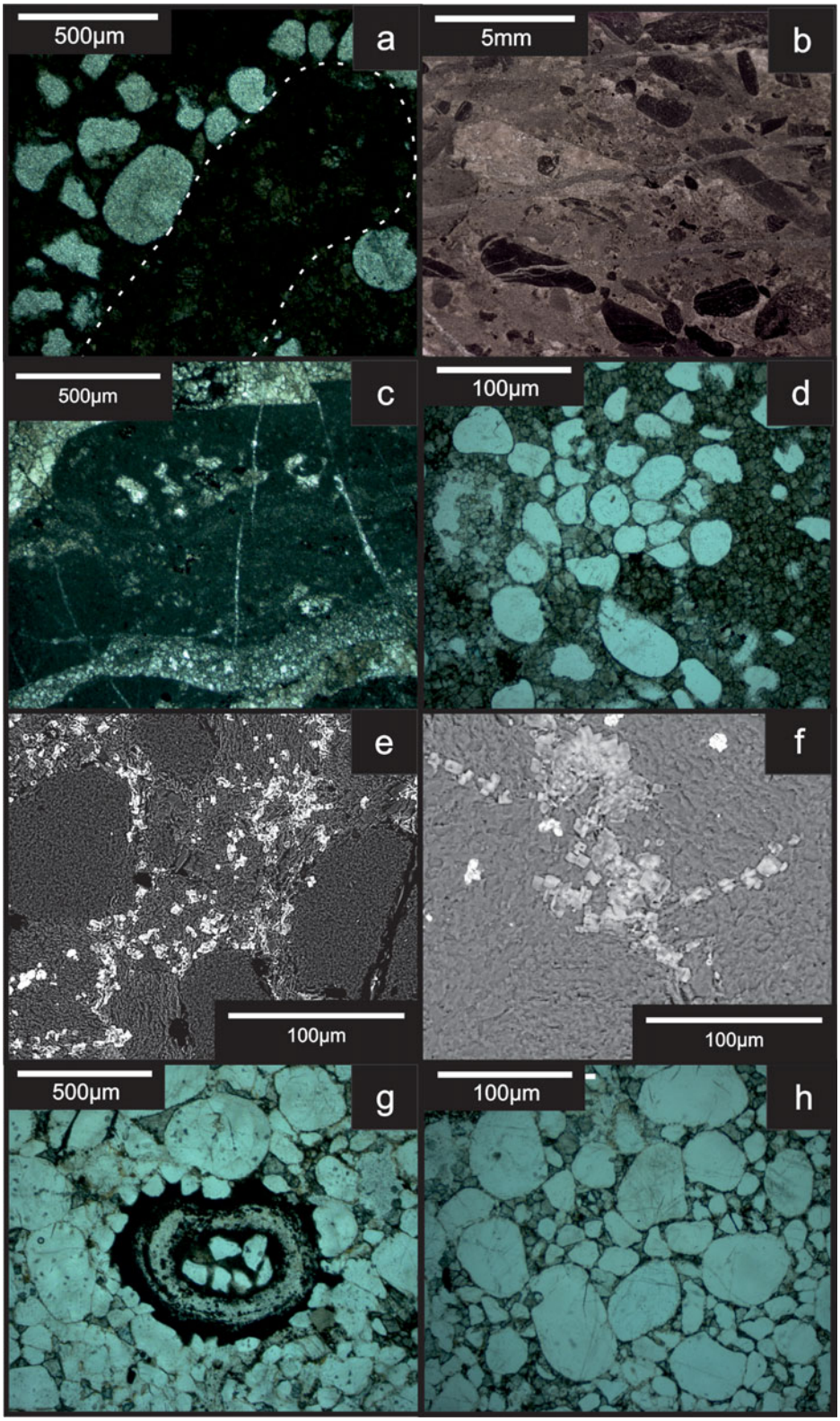


Figure 3. (Colour online) Photomicrographs of Ghrudaidh Formation facies. (a) Dolosparite pebble (highlighted with dotted line) in a sandy dolomicrite matrix, LE17. (b) Scan of slide of rudaceous limestone, exhibiting well-rounded, micrite clasts in a dolosparite matrix. (c) Rudaceous limestone of bed LE17 showing irregularly shaped, sparry bioclasts in an intraclast. (d) Photomicrograph of sandy/silty dolomite from the base of the Ghrudaidh Formation at Ardvreck Castle consisting of equal portions of rounded (aeolian) quartz grains and dolomite microspar (AC3). (e, f) Backscatter SEM images of LE6 lagoonal facies. Bright white cubes are halite, mid grey is a fine dolomite matrix and the largest, dull grey grains in (e) are aeolian quartz silt and fine sand. (g) Photomicrographs from Ardvreck Section. *Salterella* shell amongst well-rounded quartz grains of the Salterella Grit (bed AC1). (h) Rounded silt and fine sand grains, a relatively poorly sorted lithology from bed AC1.

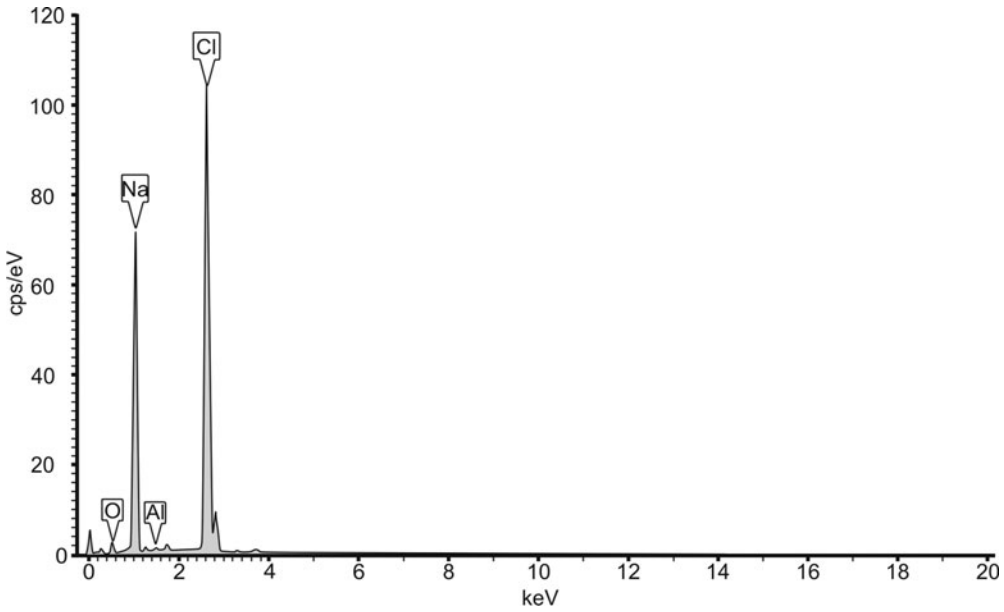


Figure 4. Representative EDS spectra taken from a halite cube in bed LE6.

*Salterella* is the only identifiable fossil in this section of the Ghrudaidh Formation, although other shell hash is also present (e.g. in LE9). The common burrows are mostly *Planolites* but there are also some branching *Thalassinoides*-like trace fossils.

The base of the Ghrudaidh Formation is taken at the sharp base of bed LE6 that marks the first appearance of carbonate. It is a dark, pyritic dolomite bed containing carbonate nodules, which in turn is succeeded by cleaved, pyritic, vuggy dolomite with *Salterella* and echinoderm fragments. SEM analysis of samples from LE6 reveals common pyrite microcrystal agglomerations ($\leq 10$ μm), scattered microcrystals and rare pyrite framboids that range in size from 5 μm to 25 μm diameter. A sample from the uppermost 8 cm of LE6 also revealed the presence of abundant tiny halite cubes, around 10 μm in diameter (Figs 3e, f, 4).

Bed LE7 is a microconglomerate bed that sits on a sharp, slightly erosive base. It grades upwards into a dolomite with common well-rounded, quartz sand grains. The well-rounded lithoclasts are up to 1 cm in diameter and consist of dolosparite. Another rudaceous horizon occurs ~ 25 m above the base of the Ghrudaidh Formation (LE17) where three thin (< 10 cm thick) erosive-based microconglomerates occur. The well-rounded equant pebbles are up to 1 cm in diameter and are composed of biomicrite (Fig. 3b). This clast lithology is not seen in the underlying beds, which are recrystallized dolostones (although they appear finer-grained and laminated in the field).

### 4.b. Ardvreck Castle

#### *4.b.1. Salterella Grit Member*

Like the strata in the Loch Eriboll section, the upper Salterella Grit Member at Ardvreck Castle is dominated by quartz arenite beds with trough cross-sets and abundant *Skolithos* burrows.

#### *4.b.2. Ghrudaidh Formation*

The contact between the Salterella Grit and Ghrudaidh Formation is sharp and is overlain by a bed (AC3) consisting in equal amounts of well-rounded quartz grains and sparry dolomite that grades upwards into less quartz-rich dolomite (AC4). This basal 1 m of the Ghrudaidh Formation is a transitional lithology that sees a decline in siliciclastic content and a transition to the pure dolomites that form the remainder of the formation. SEM examination reveals no halite crystals in these beds. The quartz-sand-bearing dolomite beds are sharply truncated by a thin microconglomerate (bed AC5) composed of small (~ 5 mm), well-rounded pebbles of dolomite in a matrix dominated by well-rounded quartz grains. The succeeding Ghrudaidh strata are dominated by beds of vuggy, burrowed, massive dolomite that dominate the remainder of the formation.

### 4.c. Interpretation

The Salterella Grit Member has been interpreted to be a tidal sandbank facies formed during a shallowing phase of deposition (McKie, 1990, 1993). Conditions alternated between periods influenced by strong tidal currents and more quiescent intervals when intense burrowing occurred. The subsequent sharp transition to the fine-grained strata at the base of the Ghrudaidh Formation at Loch Eriboll indicates a considerable decrease in depositional energy. This observation, combined with the abundant occurrence of halite and small pyrite framboids at Loch Eriboll, suggests a restricted, evaporitic lagoonal setting and low-oxygen conditions.

The persistence of the well-rounded quartz grains that dominate the Salterella Grit Member, in these basal beds of the Ghrudaidh Formation, shows that the source terrain (probably aeolian dunes on the adjacent Laurentian craton) was still nearby.

The basal Ghrudaidh strata at Ardvreck Castle differs from that at Loch Eriboll because it has a higher proportion of quartz grains and lacks evidence (such as pyrite framboids and halite) for lagoonal deposition. It is possible that this is an intertidal facies developed immediately adjacent to aeolian dunes. However, contrasting facies are seen 0.9 km to the north of the Ardvreck locality at Lochan Feòir [NC 2367 2520], where very thinly bedded, black dolomitic mudstones containing abundant *Salterella* and articulated *Olenellus* aff. *reticulatus* Peach occur in the basal Ghrudaidh Formation (Huselbee & Thomas, 1998). The Lochan Feòir strata are similar to those found at Loch Eriboll suggesting that high-energy and low-energy strata show rapid lateral changes.

The sharp truncation of the basal Ghrudaidh lagoonal/intertidal facies by a microconglomerate at both study locations is interpreted to record the passage of a zone of erosion (see sequence stratigraphic discussion in Section 6 below) and heralded the establishment of persistently well-oxygenated conditions, as shown by the bioturbation and shelly fossils in the overlying fine-grained dolostones (now mostly recrystallized). The gradual loss of rounded quartz grains upsection indicates an increasingly more distant source terrain (Raine & Smith, 2012). The low-energy conditions were occasionally punctuated by much higher energy conditions recorded by the rare oolitic strata. The frequent vuggy appearance of the strata suggests replacement of secondary evaporites as a result of concentrated pore-fluid brines. The elevated salinity is interpreted to have occurred late in the deposition of the Ghrudaidh Formation.

The bedset LE16–18 records a shift in conditions as the intensely burrowed strata is replaced by laminated dolomites and then a thin, erosive-based microconglomerate. This succession is similar to the strata that are seen at the base of the Ghrudaidh Formation where lagoonal beds were truncated during transgression.

## 5. Chemostratigraphy

This study presents the first $\delta^{13}C$ and $\delta^{18}O$ chemostratigraphic data for the Durness Group. A total of 20 samples from Ardvreck Castle were analysed, of which two samples from the Salterella Grit had insufficient carbonate content to yield a signal. In addition 40 samples from Loch Eriboll were analysed, and three were found to be too carbonate poor to yield a reliable value.

At Loch Eriboll, the lowest $\delta^{13}C_{carb}$ value is returned from the Salterella Grit Member, sample AS46, with a total inorganic carbon (TIC) of 4.5 wt % returned from *Salterella* shells. Although this is found in a sandstone we interpret the organic source of the carbonate to represent an original environmental signal. Above this, $\delta^{13}C_{carb}$ values of −3.0 ‰ occur in the silty dolomites immediately above at the base of the Ghrudaidh Formation (Fig. 5). These were followed by an increase in the overlying 10 m culminating in peak positive values of −0.4 ‰ before a decline to a broad lowpoint of −2 ‰ around 30 m above the base of the formation. The curve then swings to heavier values of −0.6 ‰ and then falls to −1.6 ‰ at the top of the Loch Eriboll section. The shorter Ardvreck Castle $\delta^{13}C_{carb}$ record (Fig. 5) shows a rapid increase across the Salterella Grit – Ghrudaidh boundary to a positive peak 2 m above before declining. The two lowest values measured from the Salterella Grit Member at the base of the section come from sandstones in which the main carbonate content is the shells of *Salterella* (carbonate content ranges from 1 to 7 wt %, see Table 1). The positive hump of $\delta^{13}C_{carb}$ values is seen at both locations and is considered to record the same chemostratigraphic event. However, at Ardvreck Castle this excursion occurs over a shorter interval (Fig. 5), an observation we attribute to a more condensed section at this location.

The $\delta^{18}O_{carb}$ values at both the Loch Eriboll and Ardvreck Castle locations show slight covariance with $\delta^{13}C_{carb}$ values only in samples taken from the Salterella Grit Member (Fig. 5 inset). The two lightest $\delta^{18}O_{carb}$ values that also correspond with the lightest $\delta^{13}C_{carb}$ values (Fig. 5) are from the sandstones of the Salterella Grit at Ardvreck Castle (see Table 1). In this member the main source of carbonate is the shells of *Salterella* and the carbonate content is significant enough (1–8 wt % TIC) to measure a carbonate carbon isotope signal. Whilst it is possible that this slight covariation is a reflection of an early diagenetic signal, at Loch Eriboll the strong similarity between Salterella Grit $\delta^{13}C_{carb}$ values (−2.98 ‰) and basal Ghrudaidh Formation values (−2.84 ‰) suggests that the Salterella Grit lowest data point at Loch Eriboll is in accordance with a reliable primary isotopic signal from the Ghrudaidh Formation. This observation suggests that $\delta^{13}C_{carb}$ values have not been affected by significant diagenesis and that the returning limb of the ROECE recorded within the Salterella Grit and immediately above in the Ghrudaidh Formation is a primary record of oceanic carbon isotope fluctuations.

The $\delta^{13}C_{org}$ record we obtained (Table 1) shows frequent oscillations with no consistent trends between the sections nor any similarity with the $\delta^{13}C_{carb}$ curve. This variability probably relates to the extremely low total organic carbon values (mostly < 0.5 %) and the likelihood that values are influenced by factors such as reworked, detrital organic carbon.

### 5.a. Interpretation

Global oscillations in the Cambrian $\delta^{13}C_{carb}$ record include the ROECE, a major negative excursion developed around the Series 2 – Series 3 boundary during which values drop to −4 ‰ followed by a rapid recovery to heavier values (Montañez *et al.* 2000;

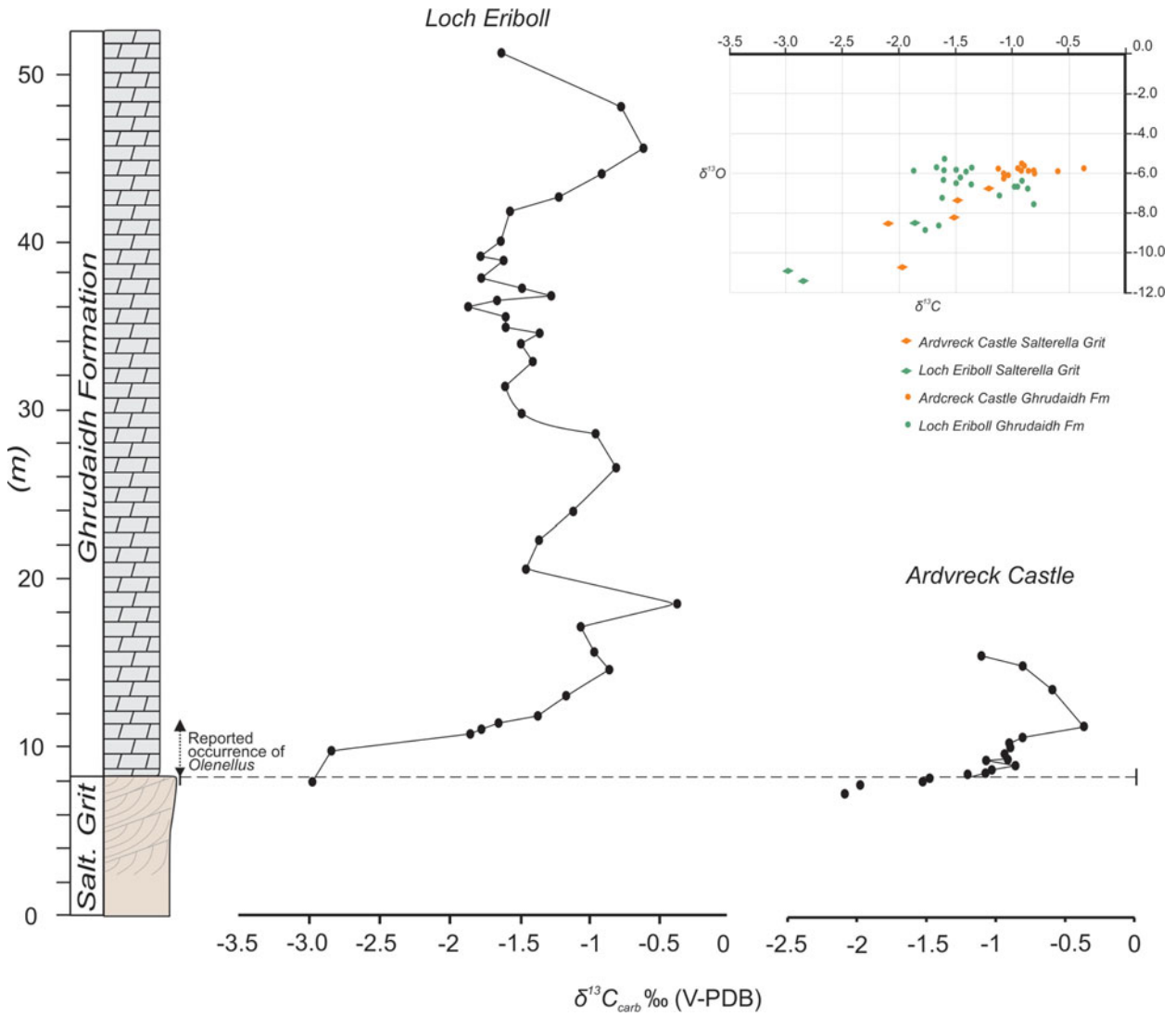


Figure 5. (Colour online) $\delta^{13}C_{carb}$ chemostratigraphic curve from Loch Eriboll and Ardvreck sections. Top right inset is a cross-plot of C and O data with samples from the Salterella Grit Member and Ghrudaidh Fm from each location delineated by respective symbols. The reported occurrence of *Olenellus* is from Huselbee & Thomas (1998); the precise location of the specimen is unknown but is indicated by dashed line.

Guo *et al*. 2010). From the Scottish data, we interpret the abrupt rise of $\delta^{13}C_{carb}$ at the base of the Ghrudaidh Formation to record this recovery phase. The amplitude of the ROECE varies considerably between regions. Laurentian values are around 4.5 ‰, in China it can reach 7 ‰ but in Siberia it is only 1.5 ‰ (Wang *et al*. 2011). In Scotland the excursion is 3 ‰, but this is likely not the full amplitude because the lowpoint of the curve is not recorded in the carbonate-free clastic sediments of the lower Salterella Grit.

The oscillations of $\delta^{13}C_{carb}$ values within the higher levels of the Ghrudaidh Formation (only studied at Loch Eriboll) can be closely matched with the global curve (Fig. 6) and they suggest that the prolonged lowpoint of values ~ 30 m above the base of the Ghrudaidh Formation (beds LE16–18) could be the DICE, an excursion that marks the Stage 5 – Drumian Stage age. As with the ROECE, the DICE varies considerably in magnitude. In South China it ranges from 1.0 to 2.5 ‰ but in the Great Basin of the western United States it is present as a 3.5 ‰ negative excursion (Zhu *et al*. 2004; Howley & Jiang, 2010). The larger values in the USA may reflect the exacerbation of the excursion by regional factors such as upwelling of deep oceanic waters and/or erosion from newly uplifted mountains (Howley & Jiang, 2010). The amplitude of the DICE in Scotland is towards the lower end of this reported range, with a magnitude of ~ 1 ‰.

Our chemostratigraphic age assignment for the Ghrudaidh Formation is also supported by the modest biostratigraphic data that is available. The single *Olenellus* reported from basal beds of the Ghrudaidh Formation (Huselbee & Thomas, 1998) indicates a late Series 2 age. The presence of *Salterella* up to 10 m above the base of the formation also indicates a Series 2 age (Fritz & Yochelson, 1988; Wright & Knight, 1995). No other biostratigraphically useful fossils occur but Wright & Knight (1995) argued that the higher levels of the Ghrudaidh Formation correlated with the Bridge Cove Member of the March Point Formation in

Table 1. Geochemical data from both Loch Eriboll and Ardvreck Castle locations. Height is measured from the base of logged sections (Fig. 2).

| | Original ID | Lithology | Height (m) | $\delta^{13}C_{carb}$ mean ‰ (VPDB) | $\delta^{18}O_{carb}$ mean ‰ (VPDB) | $\delta^{13}C_{org}$ ‰ (VPDB) | wt % S | wt % Total C | TOC wt % | TIC wt % |
|---|---|---|---|---|---|---|---|---|---|---|
| | | | | | Loch Eriboll | | | | | |
| Salterella Grit | AS36 | Sstone | 0.10 | – | – | −25.16 | 0.096 | 0.088 | 0.08 | 0.006 |
| | AS37 | Sstone | 0.50 | – | – | −25.29 | 0.166 | 0.083 | 0.09 | −0.010 |
| | AS38 | Sstone | 1.00 | – | – | −23.84 | 0.229 | 0.844 | 0.03 | 0.815 |
| | AS39 | Sstone | 1.75 | – | – | −25.70 | 0.063 | 0.059 | 0.01 | 0.051 |
| | AS40 | Sstone | 3.70 | – | – | −25.64 | 0.060 | 0.051 | 0.01 | 0.045 |
| | AS41 | Sstone | 3.80 | – | – | −25.79 | 0.054 | 0.114 | 0.08 | 0.031 |
| | AS42 | Sstone | 4.50 | – | – | −26.40 | 0.324 | 0.030 | 0.02 | 0.015 |
| | AS43 | Sstone | 5.75 | – | – | −25.95 | 0.040 | 0.036 | 0.01 | 0.026 |
| | AS44 | Sstone | 7.50 | – | – | −24.61 | 0.138 | 1.841 | 0.02 | 1.824 |
| | AS45 | Sstone | 8.25 | – | – | −24.46 | 0.354 | 6.644 | 0.10 | 6.539 |
| | AS46 | Sstone | 8.80 | −2.98 | −10.93 | −22.89 | 0.515 | 4.829 | 0.09 | 4.734 |
| | AS47 | Sstone | 9.15 | – | – | −23.81 | 0.377 | 4.353 | 0.23 | 4.119 |
| Ghrudaidh Formation | AS48 | Carbonate | 9.75 | −2.84 | −11.43 | −23.75 | 0.734 | 3.985 | 0.20 | 3.786 |
| | AS49 | Carbonate | 10.10 | – | – | −24.76 | 0.066 | 9.741 | 0.45 | 9.296 |
| | AS50 | Carbonate | 10.75 | −1.85 | −8.52 | −24.73 | −0.002 | 8.819 | 0.11 | 8.709 |
| | AS51 | Carbonate | 10.95 | – | – | −25.04 | −0.001 | 10.393 | 0.12 | 10.270 |
| | AS52 | Carbonate | 11.05 | −1.77 | −8.99 | −24.50 | −0.001 | 8.182 | 0.31 | 7.877 |
| | AS53 | Carbonate | 11.40 | −1.65 | −8.84 | −25.64 | −0.001 | 11.057 | 0.55 | 10.508 |
| | AS54 | Carbonate | 11.80 | −1.37 | −8.65 | −22.61 | −0.001 | 12.710 | 0.68 | 12.031 |
| | AS55 | Carbonate | 12.25 | – | – | −23.36 | −0.002 | 13.128 | – | – |
| | AS56 | Carbonate | 13.00 | −1.17 | −7.83 | −24.91 | −0.001 | 13.009 | – | – |
| | AS57 | Carbonate | 13.50 | – | – | −24.71 | 0.000 | 12.876 | 0.23 | 12.648 |
| | AS58 | Carbonate | 14.55 | −0.86 | −6.82 | −23.23 | 0.027 | 13.166 | 0.88 | 12.290 |
| | AS59 | Carbonate | 15.60 | −0.97 | −6.77 | −21.34 | 0.000 | 12.513 | 0.18 | 12.330 |
| | AS60 | Carbonate | 17.10 | −1.06 | −6.65 | −24.34 | −0.002 | 13.592 | 0.67 | 12.923 |
| | AS61 | Carbonate | 18.00 | – | – | −24.80 | −0.001 | 13.326 | 0.72 | 12.606 |
| | AS62 | Carbonate | 18.50 | −0.38 | −7.01 | −23.47 | −0.001 | 12.930 | 0.44 | 12.490 |
| | AS63 | Carbonate | 20.00 | – | – | −25.65 | 0.026 | 13.557 | 0.84 | 12.717 |
| | AS64 | Carbonate | 20.55 | −1.45 | −6.36 | −27.86 | −0.002 | 14.057 | 0.91 | 13.149 |
| | AS65 | Carbonate | 22.25 | −1.36 | −6.20 | −25.84 | 0.006 | 13.516 | 1.61 | 11.908 |
| | AS66 | Carbonate | 22.25 | −1.11 | −6.54 | −26.87 | 0.003 | 14.281 | 2.58 | 11.705 |
| | AS67 | Carbonate | 26.50 | −0.81 | −7.12 | −24.53 | 0.002 | 13.680 | 4.17 | 9.514 |
| | AS32 | Carbonate | 28.55 | −0.96 | −7.55 | – | 0.004 | 14.043 | 0.00 | 14.041 |
| | AS33 | Carbonate | 28.55 | −1.48 | −6.67 | – | 0.014 | 13.937 | 5.16 | 8.780 |
| | AS34 | Carbonate | 31.35 | −1.60 | −5.82 | – | −0.003 | 13.889 | 4.08 | 9.812 |
| | AS35 | Carbonate | 31.35 | −1.41 | −6.28 | −23.07 | 0.019 | 13.171 | 0.58 | 12.588 |
| | AS1 | Carbonate | 33.90 | −1.49 | −5.91 | −27.05 | −0.001 | 13.863 | 1.58 | 12.280 |
| | AS2 | Carbonate | 34.50 | −1.36 | −6.50 | – | 0.007 | 13.920 | 0.00 | 13.918 |
| | AS3 | Carbonate | 34.90 | −1.60 | −5.81 | −25.67 | −0.008 | 14.043 | 0.81 | 13.236 |
| | AS4 | Carbonate | 35.50 | −1.60 | −5.28 | −24.63 | 0.004 | 13.342 | 0.96 | 12.378 |
| | AS5 | Carbonate | 36.10 | −1.87 | −5.86 | −23.37 | 0.010 | 13.473 | 1.37 | 12.108 |
| | AS6 | Carbonate | 36.10 | −1.66 | −5.90 | – | −0.001 | 13.513 | 0.00 | 13.512 |

Table 1. Continued

| | Original ID | Lithology | Height (m) | $\delta^{13}C_{carb}$ mean ‰ (VPDB) | $\delta^{18}O_{carb}$ mean ‰ (VPDB) | $\delta^{13}C_{org}$ ‰ (VPDB) | wt % S | wt % Total C | TOC wt % | TIC wt % |
|---|---|---|---|---|---|---|---|---|---|---|
| | | | | | Loch Eriboll | | | | | |
| | AS7 | Carbonate | 36.75 | −1.27 | −5.70 | −26.17 | 0.011 | 12.828 | 1.53 | 11.299 |
| | AS8 | Carbonate | 37.05 | – | – | −25.67 | 0.012 | 12.130 | 0.95 | 11.180 |
| | AS9.1 | Carbonate | 37.20 | −1.48 | −5.71 | −26.72 | −0.002 | 12.906 | 2.39 | 10.521 |
| | AS11 | Carbonate | 37.40 | – | – | −25.98 | −0.001 | 13.093 | 1.42 | 11.673 |
| | AS12 | Carbonate | 37.80 | −1.77 | −6.76 | −25.75 | −0.009 | 12.490 | 1.05 | 11.442 |
| | AS13 | Carbonate | 38.50 | – | – | −22.82 | 0.005 | 13.284 | 1.35 | 11.931 |
| | AS14 | Carbonate | 38.85 | −1.61 | −6.17 | −23.87 | 0.010 | 13.644 | 1.18 | 12.469 |
| | AS15 | Carbonate | 39.10 | −1.78 | −7.22 | −22.20 | −0.001 | 13.405 | 2.08 | 11.321 |
| | AS16 | Carbonate | 39.55 | – | – | −21.92 | −0.006 | 13.869 | 1.60 | 12.274 |
| | AS17 | Carbonate | 40.00 | −1.63 | −6.40 | −20.15 | −0.002 | 13.859 | 2.17 | 11.693 |
| | AS18 | Carbonate | 40.95 | – | – | – | −0.001 | 13.875 | – | – |
| | AS19 | Carbonate | 41.75 | −1.57 | −6.60 | −20.72 | −0.002 | 13.767 | 5.19 | 8.577 |
| | AS20 | Carbonate | 42.20 | – | – | −24.31 | 0.000 | 13.850 | 0.62 | 13.226 |
| | AS21 | Carbonate | 42.60 | −1.22 | −6.17 | −25.47 | 0.000 | 13.679 | 0.72 | 12.959 |
| | AS22 | Carbonate | 43.50 | – | – | −25.63 | 0.005 | 13.802 | 0.11 | 13.693 |
| | AS23 | Carbonate | 44.00 | −0.91 | −6.60 | −25.00 | 0.002 | 13.925 | 0.12 | 13.804 |
| | AS24 | Carbonate | 45.50 | −0.62 | −6.39 | −25.57 | −0.002 | 13.599 | 0.29 | 13.311 |
| | AS25 | Carbonate | 47.00 | – | – | −22.53 | 0.003 | 13.774 | 1.15 | 12.621 |
| | AS26 | Carbonate | 48.00 | −0.78 | −6.63 | −20.93 | −0.001 | 13.972 | 0.23 | 13.742 |
| | AS27 | Carbonate | 49.20 | – | – | −22.21 | 0.004 | 13.974 | 0.51 | 13.462 |
| | AS29 | Carbonate | 51.20 | −1.63 | −6.63 | – | −0.002 | 13.544 | 3.91 | 9.634 |
| | AS30 | Carbonate | 52.20 | – | – | −24.97 | −0.003 | 13.385 | 0.83 | 12.554 |
| | | | | | Ardvreck Castle | | | | | |
| Salterella Grit | VR1 | Sstone | 0.50 | −2.09 | −8.55 | −27.16 | 0.122 | 1.430 | 0.04 | 1.389 |
| | VR2 | Sstone | 1.00 | – | – | −25.97 | 0.042 | 0.098 | 0.01 | 0.085 |
| | VR3 | Sstone | 2.00 | – | – | −26.26 | 0.071 | 0.050 | 0.01 | 0.038 |
| | VR4 | Sstone | 3.25 | −1.97 | −10.73 | −26.23 | 0.067 | 0.925 | 0.02 | 0.906 |
| | VR5 | Sstone | 3.50 | −1.51 | −8.24 | −26.39 | 0.019 | 6.744 | 0.06 | 6.683 |
| | VR6 | Sstone | 3.75 | −1.48 | −7.36 | −26.79 | 0.054 | 8.340 | 0.06 | 8.277 |
| | VR7 | Sstone | 4.00 | −1.20 | −6.77 | −27.03 | −0.001 | 7.516 | 0.28 | 7.239 |
| Ghrudaidh Formation | VR8 | Carbonate | 4.20 | −1.07 | −6.02 | – | 0.018 | 12.789 | – | – |
| | VR9 | Carbonate | 4.40 | −1.03 | −6.08 | −27.51 | 0.013 | 12.920 | 0.44 | 12.479 |
| | VR10 | Carbonate | 4.60 | −0.86 | −5.92 | −27.21 | 0.011 | 12.802 | 0.39 | 12.415 |
| | VR11 | Carbonate | 4.80 | −1.08 | −6.28 | −26.68 | −0.003 | 8.085 | 0.08 | 8.008 |
| | VR12 | Carbonate | 4.95 | −0.92 | −5.87 | −26.78 | −0.001 | 12.514 | 0.26 | 12.256 |
| | VR13 | Carbonate | 5.10 | −0.93 | −5.80 | −26.82 | 0.021 | 12.626 | 0.25 | 12.376 |
| | VR14 | Carbonate | 5.45 | −0.90 | −5.62 | −27.44 | −0.002 | 12.333 | 0.32 | 12.016 |
| | VR15 | Carbonate | 5.65 | −0.90 | −5.58 | −26.84 | −0.001 | 13.010 | 0.37 | 12.642 |
| | VR16 | Carbonate | 5.95 | −0.81 | −5.93 | −27.34 | 0.022 | 12.299 | 0.30 | 12.003 |
| | VR17 | Carbonate | 6.50 | −0.36 | −5.80 | −27.28 | −0.002 | 12.781 | 0.65 | 12.134 |
| | VR18 | Carbonate | 8.25 | −0.59 | −5.93 | −26.20 | −0.001 | 12.894 | 0.99 | 11.907 |
| | VR19 | Carbonate | 9.50 | −0.80 | −6.01 | −26.87 | −0.001 | 12.663 | 0.47 | 12.193 |
| | VR20 | Carbonate | 10.00 | −1.12 | −5.76 | −27.62 | −0.001 | 12.933 | 0.41 | 12.522 |

TOC – total organic carbon; TIC – total inorganic carbon.

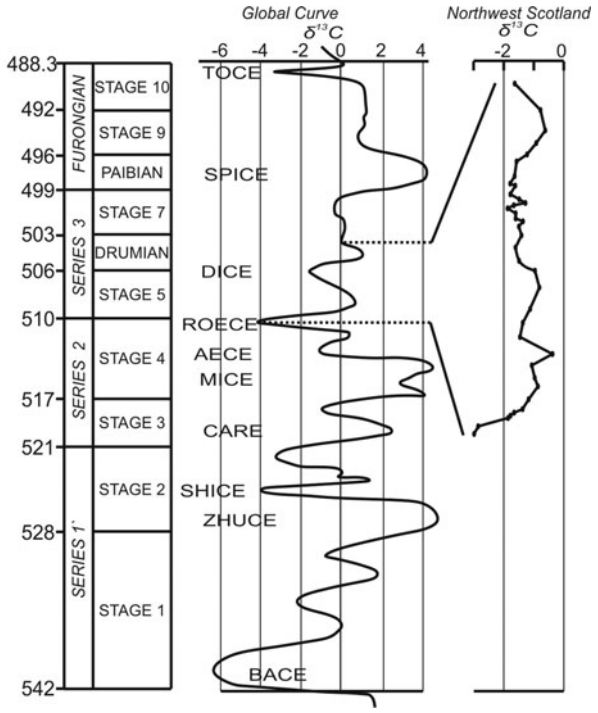


Figure 6. Global Cambrian carbon isotope curve (Zhu, Babcock & Peng, 2006) showing the proposed correlation with the Scottish sections.

western Newfoundland. This age assignment places the Scottish strata above the 10 m level in our logs within the early part of Series 3. This is in agreement with our recognition of the DICE 30 m above the base of the Ghrudaidh Formation at Loch Eriboll.

## 6. Sequence stratigraphy

The sequence stratigraphy of the Cambro-Ordovician succession of NW Scotland was discussed by Raine & Smith (2012) who placed the boundary between Sloss's (1963) Sauk I and Sauk II supersequences at the An t-Sròn–Ghrudaidh formational boundary. In North America, this supersequence boundary is a major hiatal surface that formed during the Hawke Bay event (Wright & Knight, 1995), but it is not clearly manifested outside of Laurentia (e.g. Álvaro & Debrenne, 2010; Pratt & Bordonaro, 2014). NW Scotland lay on the Laurentian margin and so this shallow-water setting might be expected to show a well-developed sequence boundary. However, the effect of the Hawke Bay event was surprisingly subdued. The formational boundary marks the culmination of prolonged shallowing and sees the transition from open, inner shelf conditions of the uppermost Salterella Grit to the restricted, lagoonal and intertidal facies of the basal Ghrudaidh Formation. This base-level shift, from inner shelf to lagoon, is probably no more than 10 m. A few metres higher a ravinement surface marks the onset of flooding and modest deepening; again, base-level changes are only of the order of a few metres. There are two options for the placement of a sequence boundary in this succession. The first would place it at the formational contact. This would imply that the overlying lagoonal/intertidal facies are a thin development of a lowstand systems tract with its top boundary being an initial flooding (ravinement) surface. The second option would consider the ravinement surface to be amalgamated with a sequence boundary and with the formational boundary only recording a facies change. Given the overall inner platform setting of the Scottish outcrops it is perhaps unlikely that any lowstand strata would be developed, because such sediment packages are typically found distally in offshore/shelf margin locations. Therefore, we consider the second option to be the most probable. Thus, the sequence boundary is developed low in the Ghrudaidh Formation and not at its base. It is likely to record a major hiatus. The halite crystals developed immediately below the surface at Loch Eriboll may have grown during this non-depositional episode in a supratidal setting. The succeeding 20 m thick succession of dolomicrites do not record major facies changes but the significant upsection decline of terrigenous material suggests continued transgression and flooding of the hinterland.

The next major facies change is centred on another thin microconglomerate (bed LE17). It is similar to the lower examples, and is also interpreted to have formed during ravinement. By comparison with the basal Ghrudaidh Formation, the finely laminated strata that underlie this bed (LE16) may be highstand lagoonal facies. Thus, this succession of beds (LE16–18), chemostratigraphically correlated with the Stage 5 – Drumian boundary, probably records the regressive–transgressive couplet seen elsewhere in the world at this level (e.g. Montañez *et al*. 1996; Babcock *et al.* 2004; Álvaro *et al*. 2013).

## 7. Conclusions

The NW Scotland sections reveal a clear sequence of events across the Series 2 – Series 3 boundary and help evaluate some of the cause-and-effect relationships of this dynamic interval.

The later part of the ROECE is preserved in the $\delta^{13}C_{carb}$ record of the basal Ghrudaidh Formation with the lowpoint of this excursion probably occurring earlier during deposition of the Salterella Grit Member. Sequence boundary formation (perhaps the equivalent of the Hawke Bay event in North America) led to the development of an erosive surface by ravinement processes that is mantled by a thin conglomerate near the base of the Ghrudaidh Formation. The overlying strata records transgression with an increasingly distal hinterland supply. No lowstand facies are developed because of the proximal setting on this Laurentian platform. The formational boundary, 2 m below the sequence boundary, is interpreted to be simply a facies contact that marks coastal progradation with inner shelf tidal clastic facies replaced by intertidal clastic sediments and dolomitic lagoonal facies.

The Stage 5 – Drumian boundary, identified from carbon isotope oscillations (DICE), is found within

the upper Ghrudaidh Formation and this too records an amalgamated sequence boundary/flooding surface with lagoonal facies transgressed by a conglomerate developed on a ravinement surface. The base of the Drumian in Gondwana is marked by the spread of anoxic facies by marine transgression (Álvaro *et al.* 2013). This level is also associated with trilobite turnover but the lack of fossils in the Scottish strata does not permit evaluation of this event. However, elsewhere in the world the earliest Drumian saw a major transgression and spread of anoxic facies, especially in Gondwanan sections (Álvaro *et al.* 2013). From our section at Loch Eriboll the dark grey, laminated dolomites (LE18) could be a Laurentian development of this transgressive anoxic phase.

*Olenellus* occurs in the basal Ghrudaidh Formation within the highstand facies, but below the sequence boundary. Thus, the ROECE extinctions, which removed the olenellids, may have post-dated the peak negative values of the ROECE. A similar post-excursion extinction of redlichiid trilobites is also seen in South China (Montañez *et al*. 2000; Zhu *et al*. 2004; Peng, Babcock & Cooper, 2012). This has a bearing on proposed extinction mechanisms. Montañez *et al*. (2000) argued that the incursion of deep anoxic waters (with a light carbon isotope signature derived from remineralized organic matter) into shallower waters may have triggered a biomass crash and trilobite extinction. The mistiming of the ROECE and extinctions in Scotland (and also in China, e.g. Zhu *et al.* 2004) does not support this scenario. However, trilobites are exceptionally rare in the Ghrudaidh Formation and it is possible that the occasional *Olenellus* fossils are holdovers that post-date the main extinction. Further collecting is required in more fossiliferous sections worldwide to fully evaluate this extinction event.

**Acknowledgements.** This research was made possible by a NERC postgraduate studentship and a postgraduate Student Bursary grant (March 2014) from the Mineralogical Society of Great Britain and Ireland and the use of the Stable Isotope Laboratory at Friedrich-Alexander University, Erlangen-Nürnberg. We thank two anonymous reviewers for their feedback.

## References

AHLBERG, P. E. R., AXHEIMER, N., BABCOCK, L. E., ERIKSSON, M. E., SCHMITZ, B. & TERFELT, F. 2009. Cambrian high-resolution biostratigraphy and carbon isotope chemostratigraphy in Scania, Sweden: first record of the SPICE and DICE excursions in Scandinavia. *Lethaia* **42**, 2–16.

ÁLVARO, J. J., AHLBERG, P., BABCOCK, L. E., BORDONARO, O. L., CHOI, D. K., COOPER, R. A. & JAGO, J. B. 2013. Global Cambrian trilobite palaeobiogeography assessed using parsimony analysis of endemicity. *Geological Society of London, Memoirs* **38**, 273–96.

ÁLVARO, J. J., BAULUZ, B., SUBÍAS, I., PIERRE, C. & VIZCAÏNO, D. 2008. Carbon chemostratigraphy of the Cambrian–Ordovician transition in a midlatitude mixed platform, Montagne Noire, France. *Geological Society of America Bulletin* **120**, 962–75.

ÁLVARO, J. J. & DEBRENNE, F. 2010. The Great Atlasian Reef complex: an early Cambrian subtropical fringing belt that bordered West Gondwana. *Palaeogeography, Palaeoclimatology, Palaeoecology* **294**, 120–32.

BABCOCK, L. E., REES, M. N., ROBISON, R. A., LANGENBURG, E. S. & PENG, S. 2004. Potential Global Standard Stratotype-section and Point (GSSP) for a Cambrian stage boundary defined by the first appearance of the trilobite *Ptychagnostus atavus*, Drum Mountains, Utah, USA. *Geobios* **37**, 149–58.

BABCOCK, L. E., ROBISON, R. A., REES, M. N., PENG, S. & SALTZMAN, M. R. 2007. The global boundary stratotype section and point (GSSP) of the Drumian Stage (Cambrian) in the Drum Mountains, Utah, USA. *Episodes* **30**, 85.

BRASIER, M. D., CORFIELD, R. M., DERRY, L. A., ROZANOV, A. Y. & ZHURAVLEV, A. Y. 1994. Multiple $\delta^{13}C$ excursions spanning the Cambrian explosion to the Botomian crisis in Siberia. *Geology* **22**, 455–8.

DEBRENNE, F., ROZANOV, A. Y. & WEBERS, G. F. 1984. Upper Cambrian Archaeocyatha from Antarctica. *Geological Magazine* **121**, 291–9.

FAN, R., DENG, S. & ZHANG, X. 2011. Significant carbon isotope excursions in the Cambrian and their implications for global correlations. *Science China Earth Sciences* **54**, 1686–95.

FRITZ, W. H. & YOCHELSON, E. L. 1988. The status of *Salterella* as a Lower Cambrian index fossil. *Canadian Journal of Earth Sciences* **25**, 403–16.

GUO, Q., STRAUSS, H., LIU, C., ZHAO, Y., YANG, X., PENG, J. & YANG, H. 2010. A negative carbon isotope excursion defines the boundary from Cambrian Series 2 to Cambrian Series 3 on the Yangtze Platform, South China. *Palaeogeography, Palaeoclimatology, Palaeoecology* **285**, 143–51.

HOWLEY, R. A. & JIANG, G. 2010. The Cambrian Drumian carbon isotope excursion (DICE) in the Great Basin, western United States. *Palaeogeography, Palaeoclimatology, Palaeoecology* **296**, 138–50.

HUSELBEE, M. Y. & THOMAS, A. T. 1998. *Olenellus* and conodonts from the Durness Group, NW Scotland, and the correlation of the Durness succession. *Scottish Journal of Geology* **34**, 83–8.

ISHIKAWA, T., UENO, Y., SHU, D., LI, Y., HAN, J., GUO, J. & KOMIYA, T. 2014. The $\delta^{13}C$ excursions spanning the Cambrian explosion to the Canglangpuian mass extinction in the Three Gorges area, South China. *Gondwana Research* **25**, 1045–56.

MALOOF, A. C., PORTER, S. M., MOORE, J. L., DUDÁS, F. Ö., BOWRING, S. A., HIGGINS, J. A., FIKE, D. A. & EDDY, M. P. 2010. The earliest Cambrian record of animals and ocean geochemical change. *Geological Society of America Bulletin* **122**, 1731–74.

MCKIE, T. 1989. Barrier island to tidal shelf transition in the early Cambrian Eriboll Sandstone. *Scottish Journal of Geology* **25**, 273–93.

MCKIE, T. 1990. Tidal and storm influenced sedimentation from a Cambrian transgressive passive margin sequence. *Journal of the Geological Society, London* **147**, 785–94.

MCKIE, T. 1993. Relative sea-level changes and the development of a Cambrian transgression. *Geological Magazine* **130**, 245–56.

MONTAÑEZ, I. P., BANNER, J. L., OSLEGER, D. A., BORG, L. E. & BOSSERMAN, P. J. 1996. Integrated Sr isotope variations and sea-level history of Middle to Upper

Cambrian platform carbonates: implications for the evolution of Cambrian seawater $^{87}Sr/^{86}Sr$. *Geology* **24**, 917–20.

MONTAÑEZ, I. P., OSLEGER, D. A., BANNER, J. L., MACK, L. E. & MUSGROVE, M. 2000. Evolution of the Sr and C isotope composition of Cambrian oceans. *GSA Today* **10**, 1–7.

PALMER, A. R. 1998. Terminal early Cambrian extinction of the Olenellina: documentation from the Pioche Formation, Nevada. *Journal of Paleontology* **72**, 650–72.

PALMER, A. R. & JAMES, N. P. 1980. The Hawke Bay event: a circum-Iapetus regression near the Lower–Middle Cambrian boundary. *The Caledonides in the USA* **2**, 15–8.

PENG, S., BABCOCK, L. E. & COOPER, R. A. 2012. *The Cambrian Period*. In *The Geologic Time Scale* **2012** (eds F. M. Gradstein, G. Ogg & M. Schmitz), pp. 437–88. Oxford: Elsevier.

PEREJÓN, A., MORENO-EIRIS, E., BECHSTÄDT, T., MENÉNDEZ, S. & RODRÍGUEZ-MARTÍNEZ, M. 2012. New Bilbilian (early Cambrian) archaeocyath-rich thrombolitic microbialite from the Láncara Formation (Cantabrian Mts., northern Spain). *Journal of Iberian Geology* **38**, 313–30.

PRATT, B. R. & BORDONARO, O. L. 2014. Early middle Cambrian trilobites from La Laja Formation, Cerro El Molle, Precordillera of western Argentina. *Journal of Paleontology* **88**, 906–24.

RAINE, R. J. & SMITH, M. P. 2012. Sequence stratigraphy of the Scottish Laurentian margin and recognition of the Sauk megasequence. In *The Great American Carbonate Bank: The Geology and Economic Resources of the Cambrian–Ordovician Sauk Megasequence of Laurentia* (eds J. R. Derby, R. D. Fritz, S. A. Longacre, W. A. Morgan & C. A. Sternbach), pp. 575–98. American Association of Petroleum Geologists Memoir 98.

SLOSS, L. L. 1963. Sequences in the cratonic interior of North America. *Geological Society of America Bulletin* **74**, 93–114.

SMITH, E. F., MACDONALD, F. A., PETACH, T. A., BOLD, U. & SCHRAG, D. P. 2015. Integrated stratigraphic, geochemical, and paleontological late Ediacaran to early Cambrian records from southwestern Mongolia. *Geological Society of America Bulletin* **128**, 442–68.

WANG, X., HU, W., YAO, S., CHEN, Q. & XIE, X. 2011. Carbon and strontium isotopes and global correlation of Cambrian Series 2–Series 3 carbonate rocks in the Keping area of the northwestern Tarim Basin, NW China. *Marine and Petroleum Geology* **28**, 992–1002.

WRIGHT, D. T. & KNIGHT, I. 1995. A revised chronostratigraphy for the lower Durness Group. *Scottish Journal of Geology* **31**, 11–22.

ZHANG, W., SHI, X., JIANG, G., TANG, D. & WANG, X. 2013. Mass-occurrence of oncoids at the Cambrian Series 2–Series 3 transition: implications for microbial resurgence following an Early Cambrian extinction. *Gondwana Research* **28**, 432–50.

ZHU, M. Y., BABCOCK, L. E. & PENG, S. C. 2006. Advances in Cambrian stratigraphy and paleontology: integrating correlation techniques, paleobiology, taphonomy and paleoenvironmental reconstruction. *Palaeoworld* **15**, 217–22.

ZHU, M. Y., ZHANG, J. M., LI, G. X. & YANG, A. H. 2004. Evolution of C isotopes in the Cambrian of China: implications for Cambrian subdivision and trilobite mass extinctions. *Geobios* **37**, 287–301.

ZHURAVLEV, A. Y. & WOOD, R. A. 1996. Anoxia as the cause of the mid-Early Cambrian (Botomian) extinction event. *Geology* **24**, 311–4.